Bioorganic & Medicinal Chemistry xxx (2015) xxx–xxx

Contents lists available at ScienceDirect

Bioorganic & Medicinal Chemistry

journal homepage: www.elsevier.com/locate/bmc

Synthesis and biological evaluation of diarylthiazole derivatives as antimitotic and antivascular agents with potent antitumor activity

Fang Wang [a,†], Zhuang Yang [a,b,†], Yibin Liu [a,†], Liang Ma [a], Yuzhe Wu [a,b,†], Lin He [a], Mingfeng Shao [a], Kun Yu [a], Wenshuang Wu [a], Yuzhi Pu [a], Chunlai Nie [a], Lijuan Chen [a,*]

[a] State Key Laboratory of Biotherapy/Collaborative Innovation Center of Biotherapy, West China Hospital, Sichuan University, Chengdu, Sichuan 610041, PR China
[b] Key Laboratory of Green Chemistry and Technology of Ministry of Education, College of Chemistry, Sichuan University, 29 Wangjiang Road, Chengdu 610064, PR China

ARTICLE INFO

Article history:
Received 17 February 2015
Revised 16 April 2015
Accepted 17 April 2015
Available online xxxx

Keywords:
Combrestatatin A-4
Diarylthiazole derivative
Tumor
Microtubule

ABSTRACT

By switching position of the N and S atom in the thiazole ring which were similar to the previously reported agent 5-(4-ethoxyphenyl)-4-(3′,4′,5′-trimethoxyphenyl)thiazol-2-amine, a series of 4,5-diarylthiazole derivatives were synthesized using Friedel–Crafts reaction based on chemical modification of Combrestatatin A-4 (**CA-4**). Their antiproliferative activities were evaluated and identified as new microtubule destabilizing agents. Structure–activity relationship study indicated that compound **8a** with 3,4,5-trimethoxyphenyl group at the C-4 position and 4-ethoxyphenyl group at the C-5 position of 2-amino substituted thiazole was of the most potent inhibitory activity in this series. **8a** was found to exhibit the IC_{50} values of 8.4–26.4 nM in five human cancer cell lines, with comparable inhibition effects to **CA-4**. Moreover, **8a** showed potency as a tubulin polymerization inhibitor, with colchicine site binding ability and comparable extent of inhibition against the growth of P-glycoprotein over-expressing multidrug resistant cell lines. Mechanism studies revealed that **8a** could block the progression of cell cycle in the G2/M phase and result in cellular apoptosis in cancer cells. As a new tubulin destabilizing agent, **8a** was also found high antivascular activity as it concentration-dependently reduced the cell migration and disrupted capillary like tube formation of HUVEC cells. Furthermore, **8a** significantly suppressed the tumor growth in HCT116 and SK-OV-3 xenograft models with tumor growth inhibitory rate of 55.12% and 72.7%, respectively. Our studies highlighted that **8a** was a promising microtubule targeting antitumor agent.

1. Introduction

Microtubules, the key components of the mitotic spindles of eukaryotic cells composed of α/β-tubulin heterodimers, play a crucial role in many biological processes including cell division,[1] formation, maintenance of cell shape, cell signaling, secretion, and intracellular transport.[2] The primary role of microtubules is to form the mitotic spindle through the polymerization of tubulin, which results in the separation of chromosomal.[3] The dysfunction of microtubules simultaneously results in the cell malfunction and usually leads to cell death.[4] As microtubules present important functions in mitosis and cell division, a large number of anticancer drugs have been developed targeting microtubules.[5,6] These drugs, often regarded as antimitotic agents,[7] are generally classified into two groups: the microtubule-stabilizing agents and the microtubule-destabilizing agents.[8,9]

Combrestatatin A-4 (**CA-4**), a natural product isolated from the African willow that displays potential activity against a broad spectrum of human cancer cells due to its antitubulin activities,[10] has attracted great interest as a microtubule-destabilizing agent that bind to the colchicine-site in β-tubulin, since it represented a class of compounds that possess dual mechanism of anticancer action.[11,12] CA-4 and its derivatives not only inhibit the growth of a wide variety of human cancer cell lines but also show vascular-disrupting effects on tumor endothelial cells. This kind of agents are thus termed vascular-disrupting agents (VDAs).[13] VDAs can cause a significant shutdown in blood flow to solid tumors by selectively targeting established tumor vasculature, leading to tumor shrinkage.[14]

The simple structure and great anticancer potency make **CA-4** a very attractive lead compound for cancer treatment. A large number of derivatives of **CA-4** have been reported. According to previous studies, three important pharmacophore components of **CA-4**

* Corresponding author. Tel.: +86 28 85164063; fax: +86 28 85164060.
E-mail address: chenlijuan125@163.com (L. Chen).
† These authors contributed equally and should be considered as co-first authors.

http://dx.doi.org/10.1016/j.bmc.2015.04.055
0968-0896/

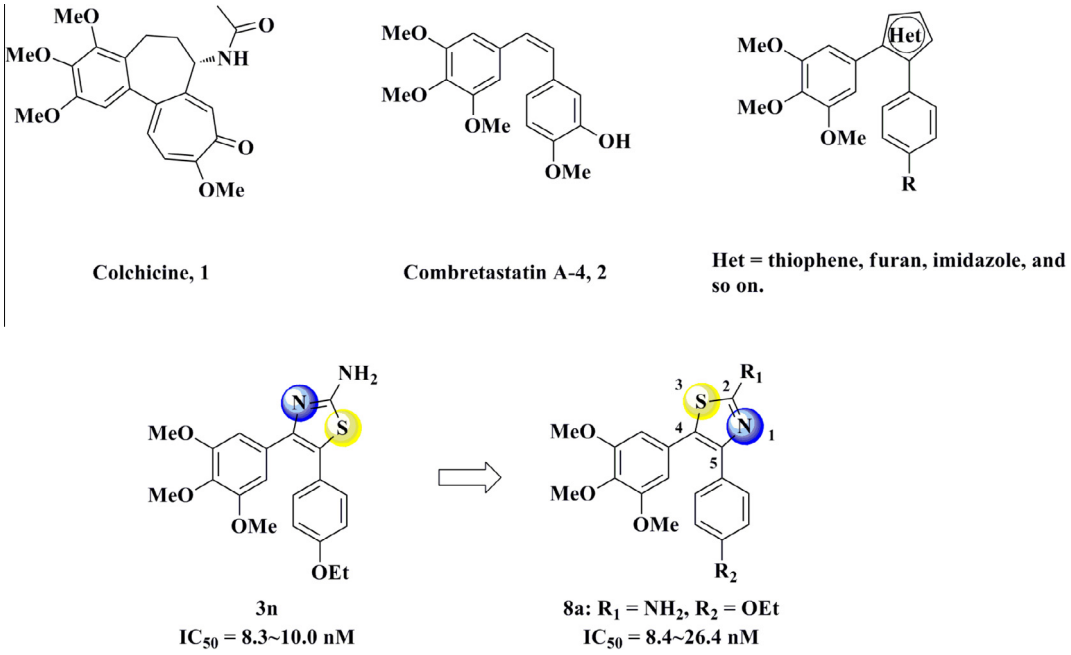

Figure 1. Tubulin interacting agents, **3n** and lead compound (**8a**).

have been reported, which are two hydrophobic phenyl rings and a vinyl in *cis* configuration bridging the two rings.[15] The restricted *cis* configuration structure can also be achieved by introducing the two phenyl ring vicinally on a suitable heterocycle such as dioxolane,[16] pyrazole, imidazole, isoxazole, oxazole, triazole, thiazole and so on.[17,18]

In a previous study, researchers have prepared a series of 2-amino-4-(3′,4′,5′-trimethoxyphenyl)-5-arythiazoles derivatives by using an efficient and versatile convergent synthetic procedure. Among them, the 5-(4-ethoxyphenyl)-4-(3′,4′,5′-trimethoxyphenyl)thiazol-2-amine (**3n**) showed the most attractive IC_{50} values against five cancer cell lines.[18] And their molecular docking studies supported that the substitution pattern on the phenyl moiety at the 5-position of the 2-amino thiazole ring played an important role for antitubulin and antiproliferative activity. Their results encouraged us to further investigate the structure–activity relationship (SAR) of this skeleton. We hypothesized that the N and S atom in the thiazole ring could help retain the correct geometric orientation of the two phenyl rings of **CA-4**, placing them at an appropriate distance for efficient interaction with the colchicine-site of tubulin.[19] In order to further investigate the effects of the position of N and S atom in the thiazole ring on the antitubulin and antiproliferative activity, we prepared a series of 5-(3′,4′,5′-trimethoxyphenyl)thiazole derivatives which were similar to **3n** but had the position of N and S atom switched (Fig. 1). In this series of designed analogues of **CA-4**, we remained the trimethoxyphenyl moiety of the A-ring, which was considered necessary for tubulin binding activity. Our modifications were mainly focused on varying substituents at the 2-position of the thiazole skeleton. Twenty-three compounds were synthesized and evaluated for their antiproliferative activity on several human tumor cell lines. Several compounds were found to show low nanomolar antiproliferative activities. Then these compounds were further evaluated for their microtubule polymerization inhibiting activity, colchicine-site binding ability and drug-resistant overcoming potency in sequence. **8a** showed the most potent activity with IC_{50}s between 8.4 and 26.4 nM in five human cancer cell lines and also showed promising activities in drug-resistant tumor cells. **8a** was further confirmed of vascular disrupting activity and in vivo antitumor activity in both HCT116 and SK-OV-3 xenograft models, suggesting that **8a** is a promising new anticancer agent to be exploited.

2. Chemistry

Starting from 2-(3′,4′,5′-trimethoxyphenyl)acetic acid (**3**), the corresponding acyl chloride **4** was prepared by the chlorination with oxalyl chloride. The following Friedel-Crafts acylation of ethoxybenzene by **4** in the presence of $AlCl_3$ gave **6a**.[20] Subsequently, the bromination of **6a** using bromine at 0 °C afforded the intermediate **7a**.[21] Finally, a series of C-2 substituted thiazole derivatives **8a–g** were obtained by the cyclization of **7a** using thiourea and its derivatives (Scheme 1). For comparison, compound **9** was synthesized using the same synthetic procedure with a *p*-methoxyphenyl substituent at the C-4 position of the thiazole ring (Scheme 1). A variety of alkyl groups were also introduced on the amine group of **8a** using sodium hydride to prepare *N*,*N*-dialkyl substituted derivatives **10a–10d** (Scheme2). Compound **10i** was prepared by the introduction of benzyl group. *N*-Acylated derivatives **10e–h** and *N*-sulfonylated derivatives **10k–o** were prepared by reacting **8a** with the sulfonylchloride. At last, **8a** reacted with ethyl isocyanate to provide **10j** with an ethyl urea at the C-2 position of the thiazole ring.[22]

3. Results and discussion

3.1. In vitro antiproliferative effects

The synthesized derivatives were evaluated for the antiproliferative effects in vitro by 3-(4, 5-dimethylthiazol-2-yl)-2, 5-diphenyltetrazolium bromide (MTT) assay against HCT116 cell (human colon cancer cell), SMMC-7221 cell (human liver cancer cell), A2780s cell (human ovarian cancer cell), HepG2 cell (human hepatocellular carcinoma cell), and SK-OV-3 cell (human ovarian cancer cell). **3n** was used as positive control.

As shown in Table 1, the compound **8a**, which interchanged the heteroatoms N and S position from **3n**, remained almost equal antiproliferative activity compared to **3n**, and the mean IC_{50} on the tested cell lines was 17.6 nM. Then the C-2 position of thiazole was replaced with different substituted groups to investigate the influence on the antiproliferative activity. As presented in Table 1, when changing the amino group of the 2-position of thiazole ring with H (**8b**), methyl (**8c**) and *t*-butyl (**8d**), the activities were decreased by the chain elongation. The introduction of electron withdrawing groups (EWG) such as diethoxymethyl group (**8e**), formyl group (**8d**) and ethyl carboxylate (**8f**)) also caused a significant decrease of the antiproliferative activity, especially **8e** and **8f**, with IC_{50}s above 5 μM. These results confirmed that the amino group at the 2-position of thiazole ring was a key structure to keep the antiproliferative activity. At the same time, the replacement of ethoxyl with methoxyl (**9**) also caused increase of the IC_{50}s.

To further explore the structure–activity relationship (SAR), different substitute amino groups were replaced by electron withdrawing groups (EWG) and electron-donating groups (EDG). When introduced dialkyl substitute groups (dimethyl **10a**, diethyl **10b**, dipropyl **10c**, diisopropyl **10d** and dibenzyl **10i**) to the amino, the IC_{50}s were all excess 5 μM. Then we introduced a series of amide, **10e**–**10h**. With the increasing of the length of alkyl chain of amide, there was a little decrease in antiproliferative activities compared to **8a**. Surprisingly, the compound of **10j**, with a urea structure, retained the activity, and the IC_{50}s of **10j** on SMMC-7721 and A2780s cells were lower than **8a**. The antiproliferative activities of the sulfonamide derivatives (**10k**–**10o**) were all above 5 μM. Those results proved that the EDG and sulfamide groups were not tolerated and the amide groups were acceptable. Hence, **8a** and several other agents were potent compounds for further pharmacological evaluation.

3.2. Microtubule polymerization inhibiting activity

To identify whether the antiproliferative activities of seven representative compounds (**8a**, **8b**, **8c**, **8f**, **10f**, **10g** and**10j**) resulted from direct interactions with tubulin, these compounds were evaluated for their tubulin destabilization effects by measuring their interaction with purified porcine–brain tubulin at protein concentration of 3 mg/mL. **CA-4** and colchicine were used as positive controls. As a result, compound **8a** was found to be the most active compound with the microtubule assembly IC_{50} of 2.736 μM. Meanwhile, **8b** and**10j** were also potent tubulin polymerization inhibiting agents with IC_{50} values ranging from 3.554 to 3.900 μM, which were better than other compounds as well as **CA-4** and colchicine. Others were somewhat less active than the above three (summarized in Fig. 2A). In good correlation with its antiproliferative effect, this trend of tubulin polymerization

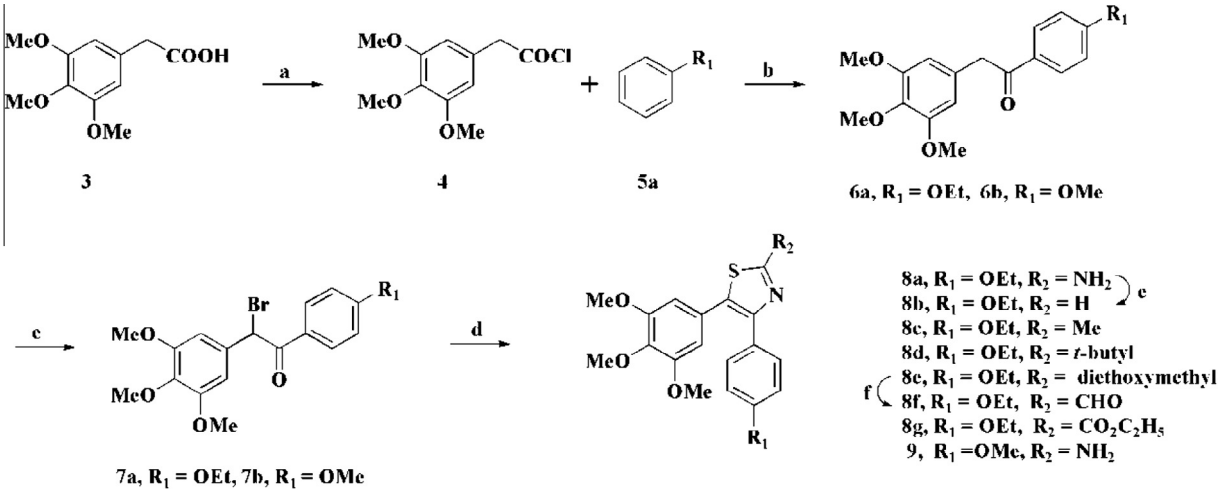

Scheme 1. Synthesis of **8a**–**9**. Reagents and conditions: (a) oxalyl chloride, DMF (2 drops), THF, rt, 40 min; (b) phenyl ethyl ether, $AlCl_3$, rt, overnight; (c) Br_2, ether, 0 °C, 40 min; (d) method for compounds **8a**, **8c**, **8d**, **8e**, **8g** and **9**: thiourea or substituted thiourea, EtOH, reflux, 3 h; (e) method for compound **8b**: isopropyl nitrite, DMF, 80 °C, 3 h; (f) Method for compound **8f**: HCl, acetone, reflux, 3 h.

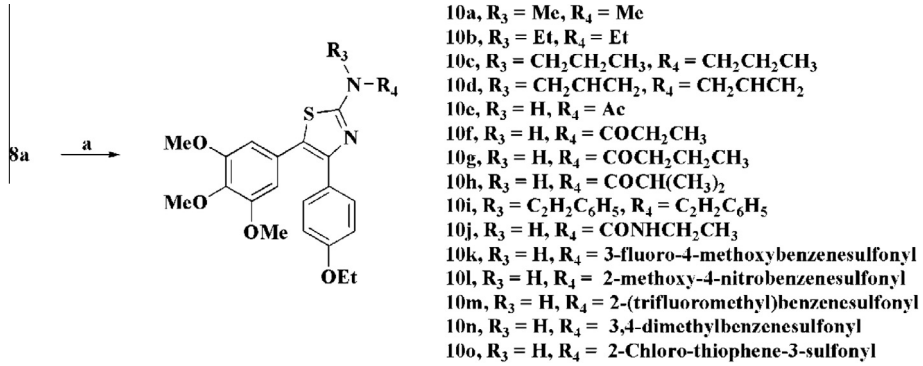

Scheme 2. Synthesis of **10a**–**10o**. Reagents and conditions: (a) method for compounds **10a**–**10d**: RI, NaH, THF, rt, 3 h; method for compounds **10e**–**10h**: anhydride, reflux, 3 h; method for compound **10i**: $C_6H_5CH_2Br$, NaH, THF, rt, 3 h; Method for compound **10j**: ethyl isocyanate, DCM, rt, 3 h; Method for compounds **10k**–**10o**: RSO_2Cl, Et_3N, DCM, 3 h.

Table 1
In vitro cell growth inhibitory effects of compounds on human tumor cell lines

Compd	IC_{50}[a] (nM)				
	HCT116	SMMC-7221	A2780s	HepG2	SK-OV-3
3n[b]	9.2 ± 2.0	10 ± 2.0	8.6 ± 2.0	8.3 ± 2.0	8.4 ± 2.0
8a	8.4 ± 2.0	23.0 ± 20.0	16.0 ± 9.0	26.4 ± 10.0	14.2 ± 8.0
8b	62.0 ± 20.0	128.0 ± 30.0	86.0 ± 40.0	65.0 ± 30.0	10.0 ± 20.0
8c	64.0 ± 20.0	126.0 ± 40.0	106.0 ± 30.0	368.0 ± 50.0	68.0 ± 10.0
8d	>5000	>5000	>5000	>5000	>5000
8e	>5000	>5000	>5000	>5000	>5000
8f	48.0 ± 60.0	106.0 ± 40.0	104.0 ± 4.0	50.0 ± 20.0	9.0 ± 30.0
8g	>5000	>5000	>5000	>5000	>5000
9	93.7 ± 20.0	9.0 ± 5.0	14.0 ± 70.0	50.6 ±2.0	110.0 ± 8.0
10a	>5000	>5000	>5000	>5000	>5000
10b	>5000	>5000	>5000	>5000	>5000
10c	>5000	>5000	>5000	>5000	>5000
10d	>5000	>5000	>5000	>5000	>5000
10e	10.2 ± 10.0	13.0 ± 3.0	10.2 ± 20.0	60.9 ± 40.0	167.0 ± 8.0
10f	50.5 ± 4.0	10.8 ± 40.0	5.1 ± 10.0	40.6 ± 20.0	60.4 ± 4.0
10g	18.0 ± 2.0	11.0 ± 4.0	18.0 ± 10.0	76.8 ± 20.0	105.2 ± 40.0
10h	22.5 ± 10.0	65.2 ± 20.0	22.5 ± 4.0	177.0 ± 10.0	85.2 ± 20.0
10i	>5000	>5000	>5000	>5000	>5000
10j	22.1 ± 10.0	10.6 ± 20.0	1.3 ± 4.0	30.7 ± 20.0	29.2 ± 8.0
10k	>5000	>5000	>5000	>5000	>5000
10l	>5000	>5000	>5000	>5000	>5000
10m	>5000	>5000	>5000	>5000	>5000
10n	>5000	>5000	>5000	>5000	>5000
10o	>5000	>5000	>5000	>5000	>5000

[a] IC_{50} = compound concentration required to inhibit tumor cell proliferation by 50%. Data are expressed as the mean ± SEM from the dose-response curves of at least three independent experiments.
[b] Use **3n** as positive control.

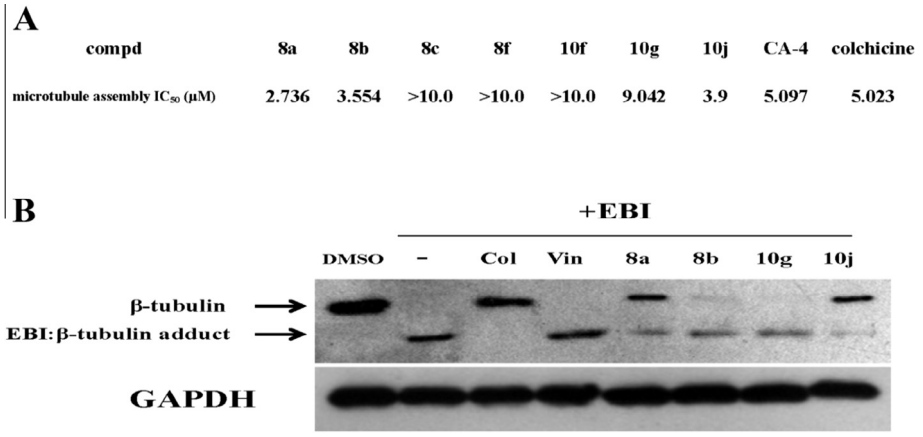

Figure 2. Inhibition of tubulin polymerization and colchicine binding by the selected compounds. (A) Effect of the selected compounds on tubulin polymerization. Tubulin was at 3 mg/mL and pre-incubated at 4 °C for 30 min, then the compounds at the indicated concentrations as well as guanosine triphosphate (GTP) were added to start the tubulin polymerization reactions. The reaction was monitored at OD340 nm at 37 °C. The microtubule assembly IC_{50} values were summarized. (B) EBI assay: HepG2 cells were treated with DMSO, colchicine (Col, 5 μM), vinblastine (Vin, 10 μM) or **8a** (5 μM), **8b** (5 μM), **10g** (5 μM), **10j** (5 μM) for 4 h. Next, EBI (100 μM) was added, and after 1.5 h, the cells were harvested and cell extracts were prepared for Western blot analysis using anti-β-tubulin antibody. EBI could result in the formation of a β-tubulin adduct (a second immunoreactive band) that migrates faster. Compounds that could pre-occupy the colchicine-site in β-tubulin prevent the formation of the EBI: β-tubulin adduct.

inhibition stated that these compounds were a group of novel microtubule de-stabilization agents.

3.3. EBI competition assay

To further confirm the binding site in tubulin of this series of agents, a recently reported and approbated N,N′-ethylene-bis(iodoacetamide) (EBI) competition assay was conducted.[11,23] In general, EBI could produce an β-tubulin adduct which could be detected by Western blot as a second immuno-reactive β-tubulin band that migrates faster than β-tubulin itself, while if EBI is added to cells previously treated with a colchicine-site binder, the EBI adduct cannot be observed. In our experiment, HepG2 cells were confirmed to be also suitable for this assay. Colchicine and selected compounds were respectively tested at the concentration of 5 μM. As shown in Figure 2B, colchicine completely inhibited the appearance of the β-tubulin adduct. **8a** and **10j** were confirmed to have the ability to bind to the colchicine-site. However, the binding affinity of **8a** and **10j** to the colchicine-site was not as strong as colchicine. At the same concentration of 5 μM, they did not totally block the observation of the second band. Such ability of two other agents, **8b** and **10g**, were even weaker. Vinblastine, a well reported

drug that has a distinct and non-overlapping binding site from colchicine, was used as a negative control at a higher concentration of 10 μM to illustrate that no false results were obtained.

3.4. Effect of 8a, 8b and 10j on multidrug resistant cells

It is well reported that microtubule targeting agents have advantage in circumventing drug resistance, that is, a long existed obstacle in cancer chemotherapy for decades.[24,25] As **8a**, **8b** and **10j** have nice microtubule de-polymerization activity, we then compared the inhibitory potency of **8a**, **8b** and **10j** on the drug-resistant and their related sensitive cancer cell lines.[26] As described in Table 2, A549/T cell line was identified as taxol resistance human lung cancer cell line with the IC_{50} of 520 nM for taxol, MCF-7/ADR and H1975 were respectively described as doxorubicin resistance human breast adenocarcinoma cell line with the IC_{50} of 5300 nM and gefitinib resistant human lung cancer cell line with the IC_{50} of 14707 nM. The cell lines of A549/T and MCF-7/ADR have been reported to express high level of P-glycoprotein (Pgp-1).[27] Compound **8a** exhibited significant cytotoxic potency against sensitive and resistant cells. The IC_{50} values of **8a** against A549, A549/T, MCF-7, MCF-7/ADR, HCC827 and H1975 cell lines were 84 nM, 43 nM, 100 nM, 190 nM, 97 nM and 217 nM, respectively. Compared with taxol and doxorubicin, **8a** had much lower resistance indexes. The resistance ratio (RR) values of **8a** were 0.51 between A549 & A549/T; 1.9 between MCF-7 & MCF-7/ADR; 2.24 between HCC827 & H1975 compared with taxol (173), Doxorubicin (241) and Gefitinib (446). Meanwhile, **10f** and **10j** also showed potent activities against these cell lines with low RR index, but their IC_{50} values were inferior compared to **8a**. The results of the antiproliferative evaluation of the synthesized compounds suggested that **8a** exerted superior anticancer activity in vitro and the activity of this series of agents was not affected by Pgp-1 over-expressing. Summing up the data above, we concluded that **8a** should be the most out-standing agent to receive further investigation.

3.5. Analysis of cell cycle and cell apoptosis

The cell cycle of a eukaryotic cell is a crucial checkpoint for chemotherapeutic drugs. To investigate whether **8a** could lead to cancer cell cycle arrest, similarly as other reported antimitotic agents, the effects of **8a** at different concentrations on cell cycle progression were examined in HCT116 and HepG2 cells by flow cytometry. As shown in Figure 3A and C, following the increase of dose of **8a**, HCT 116 cells were accumulated in the G2/M phase with a concomitant decrease of population in the G1 and S phases, and when the concentration increased to 1 μM, 79.22% of the population distributed in the G2/M phase, highlighting that **8a** dose-dependently blocked the progression of the cell cycle in the G2/M phase. Then, we tested the potency of **8a** to induce cell apoptosis by a PI & annexin-V dual-staining analysis. This method could provide discrimination between live cells (annexin-V-/PI-), early apoptotic cells (annexin-V+/PI−), late apoptotic cells (annexin-V+/PI+), and necrotic cells (annexin-V−/PI+), in which both early apoptotic and late apoptotic cells contribute to the apoptotic population. As shown in Figure 3B and D, significant apoptosis were observed after treatment with **8a**, which exhibited in a both concentration and time dependent manner. Dramatically, the populations of apoptotic cells all increased to more than 60% when the time point was 48 h, with the figure of 75.7% (43.1% + 32.6%) at the highest concentration of 1 μM. Similar results were obtained from the analysis on HepG2 cells (data shown in Supporting information).

Table 2
In vitro cell growth inhibitory effects of selected compounds on drug-resistant cell lines

		8a	8b	10j	Taxol
IC_{50}[a] (nM)	A549	84 ± 2	696 ± 213	103 ± 17	2.3 ± 0.9
	A549/T	43 ± 2	425 ± 91	140 ± 32	520 ± 45
	RR[b]	0.51	0.45	0.64	173
		8a	**8b**	**10j**	Doxorubicin
	MCF-7	100 ± 5	1160 ± 99	417 ± 20	22 ± 8
	MCF-7/ADR	190 ± 10	1559 ± 134	727 ± 150	5300 ± 400
	RR[b]	1.9	1.3	1.7	241
		8a	**8b**	**10j**	Gefitinib
	HCC827	97 ± 5	469 ± 126	623 ± 87	33 ± 1
	H1975	217 ± 28	1115 ± 77	220 ± 19	14707 ± 905
	RR[b]	2.24	2.38	0.35	446

[a] IC_{50} = compound concentration required to inhibit tumor cell proliferation by 50%. Data are expressed as the mean ± SEM from the dose-response curves of at least three independent experiments.

[b] Resistance ratio, the values express the ratio between IC_{50} determined in resistant and non-resistant cell lines.

3.6. Immunofluorescence staining of microtubule

Subsequently, we conducted an immunofluorescence assay to confirm the antimitotic property of **8a**, as immunofluorescence staining could provide an in situ observation of the microtubule system. As shown in Figure 4, we observed the normal arrangement and organization of microtubule structures without drug treatment. When treated with **8a** at the concentration of 0.2 μM for 24 h, we observed that such formation of normal microtubule was inhibited. When the concentration of **8a** increased to 0.5 μM, more serious demolishment of microtubule was detected. Moreover, from the property of the observed shape change of microtubule structure triggered by **8a**, we could verdict that the mechanism of **8a** on microtubule was inhibition of polymerization. The outcome was in accordance with the previously discussed data.

3.7. Molecular docking

Molecular docking simulations were performed on **8a** to understand the interaction model binding to tubulin protein and to rationalize our experimental findings. Figure 5 shows that the proposed binding of **8a** was also very similar to the pose of the co-crystallized DAMA-colchicine just like the previously reported compound **3n**.[18] The B ring which contained the ethoxyl group could overlap well with the seven membered ring of colchicine, and the trimethoxyphenyl ring (A ring) was placed approaching toward βCys241. The *p*-OMe formed a hydrogen bond with the residue. The bond length of this hydrogen bond was 3.42 Å. At the same time, the phenyl ring in the A ring formed a π–σ bond with Leu248. The bond length of this π–σ bond was also 3.42 Å. Thus, the scaffold occupied the active site of the protein, deeply located inside the cavity.

3.8. In vitro evaluation of antivascular activity

The concept that antimitotic agents binding to the colchicine-site in tubulin also possess vascular disrupting activity has been well established. This class of compounds could be referred as provided with dual mechanism of action affecting both tumor cells and tumor related endothelial cells. The microtubule dynamic disruption could be linked with endothelial cell shape change. We used cultured HUVEC cells to test the antivascular activity of **8a** in vitro. Firstly, we examined the antiproliferative potency of **8a** on HUVECs. The calculated IC_{50} at 48 h time point was 40.2 nM,

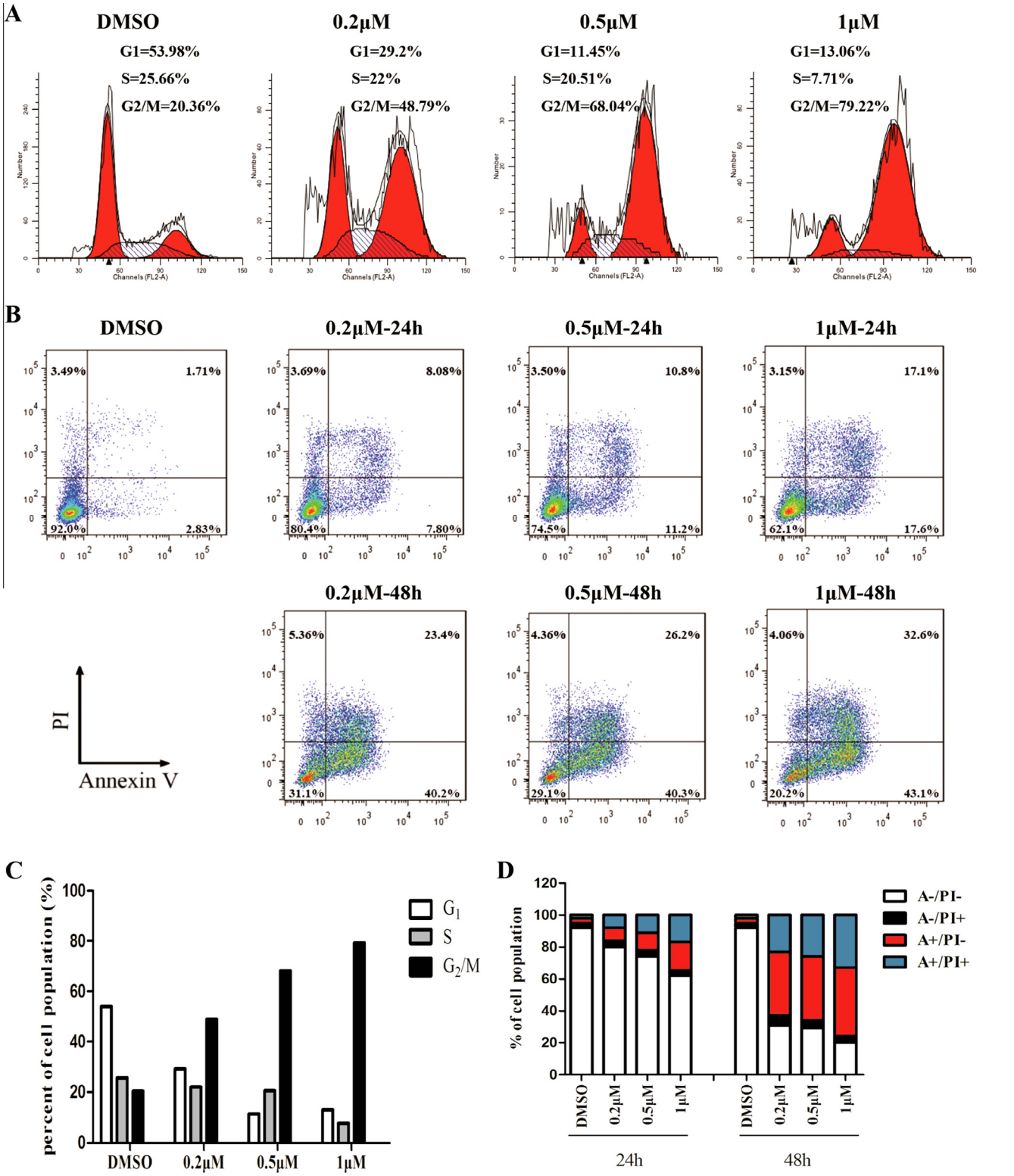

Figure 3. Analysis of cell cycle and cell apoptosis in HCT116 cells. (A) Effects of **8a** on cell cycle in HCT116 cells. Cells were treated with 0.2 μM, 0.5 μM, or 1 μM of **8a** for 24 h. (B) Flowcytometric histograms of apoptotic HCT116 cells after 24 or 48 h treatment with **8a** at the indicated concentrations. (C) Graph summarizing the cell cycle distribution effected by **8a**. (D) Graph summarizing the percentage of cells found in the different regions of the biparametric flowcytometric histograms, in which the A+/PI− and the A+/PI+ region represent the apoptotic population.

which was comparable of those on cancer cell lines. Thus, this result hinted that **8a** has the potential of disrupting the vascular network.

Logically, we set off to go on a wound-healing migration assay to assess the effect of **8a** on HUVECs migration. As shown in Figure 6A and C, **8a** could inhibit the migration of HUVECs in a dose-dependent manner. At the concentration of 500 nM, **8a** almost completely blocked the migration.

Then we also evaluated the ability of compound **8a** in a tube formation assay. After being seeded on Matrigel, HUVECs could

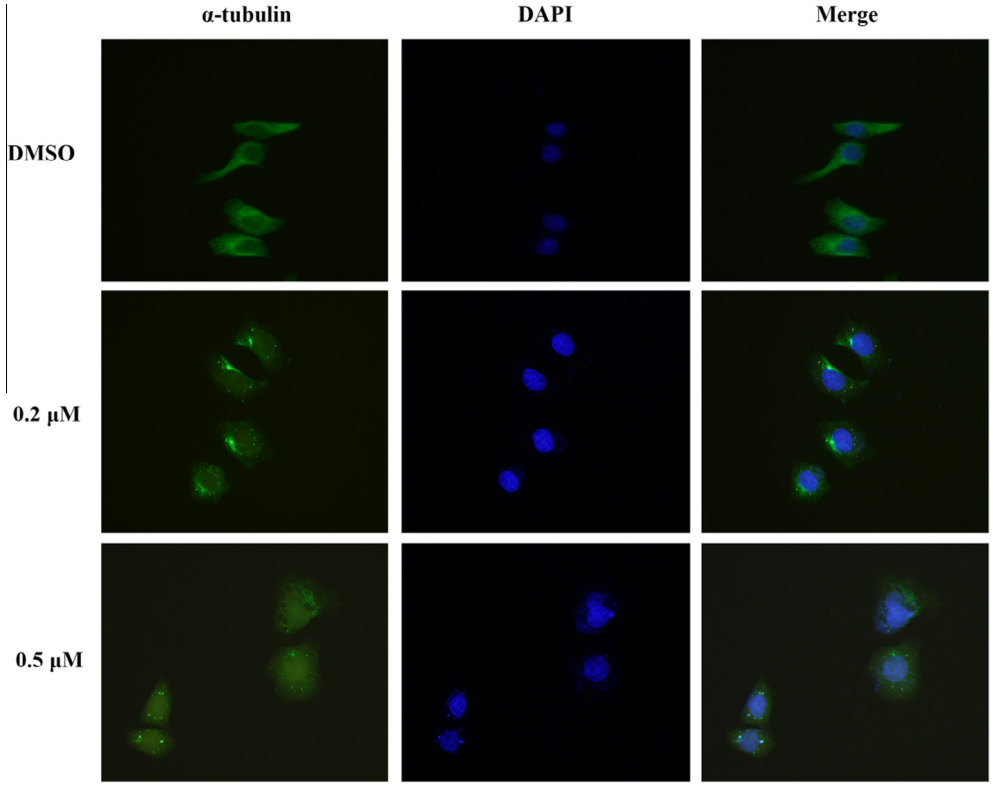

Figure 4. Effect of **8a** on the organization of cellular microtubule network. Tubulin are shown in green and the nuclei in blue.

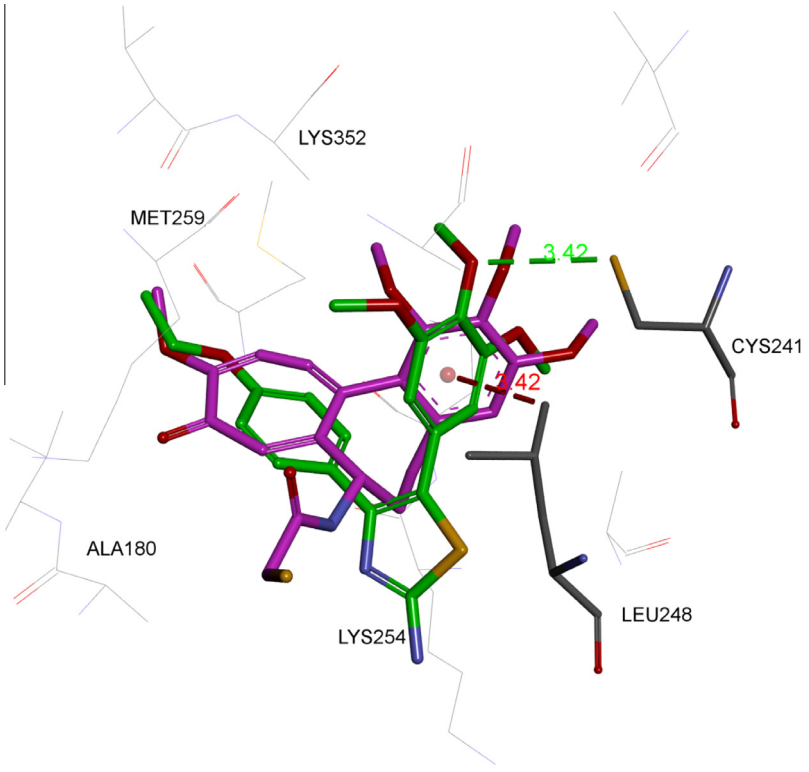

Figure 5. The close view of **8a** (green) and DAMA-colchicine (purple) in the β-tubulin binding site. The hydrogen bond (shown by a green line) and the π–σ bond (shown by a red line) were labeled.

Please cite this article in press as: Wang, F.; et al. *Bioorg. Med. Chem.* (2015), http://dx.doi.org/10.1016/j.bmc.2015.04.055

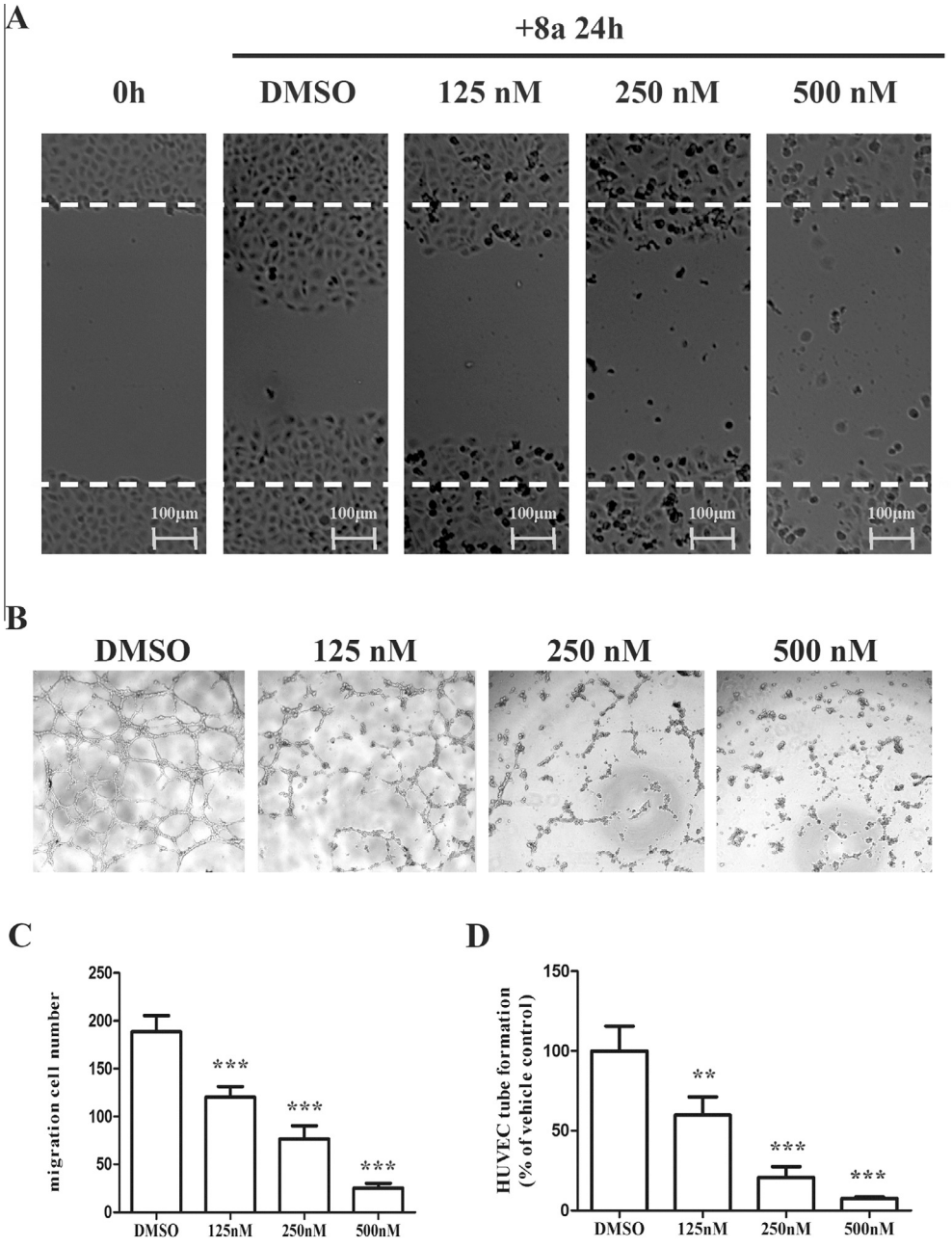

Figure 6. Effects of **8a** on the HUVECs migration and tube formation. (A) HUVECs incubated with vehicle control or the indicated concentrations of **8a** at the 0 h and 24 h time points were photographed under a phase contrast microscopy (magnification: 100×). The migrated cells from 3 separate fields were quantified by manual counting. (B) HUVECs (1×10^4 cells) suspended in EBM2 containing the indicated concentrations of **8a** were added to the Matrigel. After incubation for 8 h at 37 °C, capillary networks were photographed and quantified (magnification: 100×). (C) Statistical data of cell migration assay. Data represented the mean ± standard deviation (SD) from three fields. $^{**}P$ <0.01; $^{***}P$ <0.001; significantly different compared with control by one-way ANOVA and a post test of Tukey's multiple comparison. (D) Statistical data of tube formation assay.

form capillary-like tubules with multicentric junctions. After 8 h treatment in different concentrations (125–500 nM) of compound **8a**, the capillary-like tubes were interrupted in different levels. At the two higher concentrations of **8a**, most cells were spherical and aggregated in small clumps (Fig. 6B). Quantitative image analysis showed that **8a** markedly decreased the capillary-like tubules in a concentration-dependent manner (Fig. 6D).

3.9. In vivo antitumor activity

Due to the potent in vitro antiproliferative activity of compound **8a**, a preliminary in vivo antitumor study was conducted. We established s.c. xenograft models using two tumor cell lines (HCT116 and SK-OV-3). Once tumor volume reached a size of around 100 mm^3, **8a** was administrated intraperitoneally at doses of 20 mg/kg or 50 mg/kg daily. 5-Fluorouracil (5-FU), as positive control, was injected intraperitoneally at 10 mg/kg daily. As shown in Figure 7, **8a** dose-dependently inhibited tumor growth during the treatment. In HCT116 tumor model, tumor growth was significantly suppressed after the treatment with **8a**, which were 49.55% and 55.12% reduction at 20 mg/kg and 50 mg/kg at the end of 42 days, respectively, while 5-FU caused 37.3% reduction. Similarly, the same trend was observed in SK-OV-3 xenograft model. Tumor growth inhibition rate was 49.6% when treated with **8a** at 20 mg/kg while this rate reached 72.7% at 50 mg/kg.

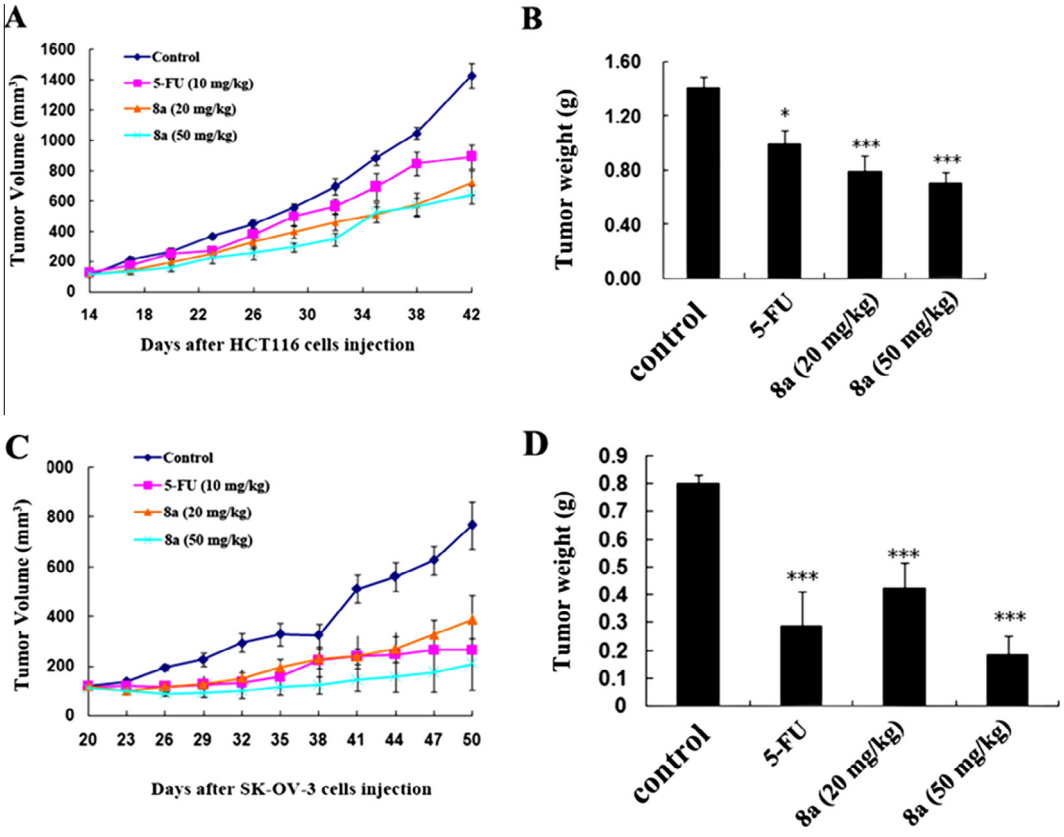

Figure 7. In vivo antitumor activity of **8a**. (A) Inhibition effect of **8a** on the HCT116 xenograft model. HCT116 tumor-bearing nude mice were intraperitoneally administered vehicle alone or 10 mg/kg of 5-FU, or **8a** at 20 mg/kg and 50 mg/kg. Each mice group contained 6 mice; bars, ±SD. (B) The bar charts of HCT116 tumor weight $^{*}P$ <0.05, $^{**}P$ <0.01 and $^{***}P$ <0.001, significantly different compared with control by one-way *ANOVA* and a post test of Tukey's multiple comparison. (C) Inhibition effect of **8a** on the SKOV-3 xenograft model. SKOV-3 tumor-bearing nude mice were administrated vehicle alone or 10 mg/kg of 5-FU, or **8a** at 20 mg/kg and 50 mg/kg. Each mice group contained 6 mice; bars, ±SD. (D) The bar charts of SK-OV-3 tumor weight.

During the experiment, body weight loss caused by **8a** at the doses of both 20 mg/kg and 50 mg/kg was detected, inferring some extent of toxicity of this agent. However, such phenomenon also appeared in the groups administrated 5-FU, a licensed drug. No other significant changes in gross measures were observed, including feeding, and animal behavior. These results suggested that **8a** could act as a potential candidate for cancer treatment.

4. Conclusion

In summary, we have synthesized a series of 4,5-diarylthiazole derivatives with the transformation of N and S atom in the thiazole ring according to the previous study. Compound **8a** showed the most potent inhibitory activity with the IC_{50} values ranging from 8.4 to 26.4 nM in the tumor cell lines (HCT116, SMMC-7221, A2780s, HepG2 and SK-OV-3). Tubulin polymerization assay and an EBI competition binding test demonstrated that **8a** inhibited tubulin polymerization in a mechanism similar to colchicine. **8a** was also verified to be effective against several multidrug resistant cancer cell lines. **8a** was further validated as a specific G2/M phase blocker and it induced apoptosis in HCT116 and HepG2 cells. In vitro immunofluorescence staining as well as molecular modeling studies confirmed the microtubule-targeting effect of **8a**. At the same time, wound-healing migration assay and tube formation assay using HUVECs showed that **8a** was manifested to possess a second mechanism of vascular disrupting ability. Then we established two in vivo xenograft tumor models (HCT116 and SK-OV-3) and **8a** possessed potent inhibitory activity. Above all, these promising results demonstrated that **8a** was a potent microtubule destabilizing and vascular disrupting agent for cancer treatment. This study suggested that the compound **8a** manifested great interaction energy with the colchicine binding site on tubulin. It is also worth noting that the results of this study discloses the possibility of designing new, more potent derivatives with improved antitumor activity and vascular disrupting activity.

5. Experimental section

5.1. Chemistry

^{1}H NMR were recorded on a Varian spectrometer (Varian, Palo Alto, CA, USA) model Gemini 400, chemical shifts are reported in ppm, relative to internal tetramethylsilane (TMS), where TMS (δ) = 0.00 ppm. The multiplicity of the signal is indicated as s, singlet; d, doublet; t, triplet; q, quartet; m, multiplet, defined as all multipeak signals where overlap or complex coupling of signals makes definitive description of peaks difficult. Reactions were monitored by analytical TLC on 0.20 mm silica gel F_{254} plates (Qingdao Ocean Chemical Factory, Shandong, China). High-resolution mass spectra were obtained by Q-TOF Priemier mass spectrometer utilizing electrospray ionization (ESI) (Micromass, Manchester, UK).

5.1.1. Procedure for the synthesis of intermediate 4

To a stirring solution of the 2-(3,4,5-trimethoxyphenyl)acetic acid (1.13 g, 5 mmol) in tetrahydrofuran(THF, 20 mL) was added oxalyl chloride (2.0 equiv). 2 Drops *N*,*N*-dimethylformamide were immediately added. After stirred for 10 min, the solution was

carefully concentrated to provide viscous oil. Fresh THF (50 mL) was added and the solution was concentrated again. The resulting oil was then placed under high vacuo for 3 h. The acid chloride was obtained without any further purification.

5.1.2. Procedure for the synthesis of 6a

The 2-(3,4,5-trimethoxyphenyl)acetyl chloride dissolved in 5 mL phenyl ethyl ether was added together with phenyl ethyl ether (5 mL) in the three-necked bottles. Then aluminum chloride (0.733 g, 0.6 mmol) was added under nitrogen at room temperature and the solution was stirred at room temperature overnight. After the reaction was completed, the mixture was poured into ice water (20 mL) and extracted with ethyl acetate (3 × 20 mL). The combined organic phase was washed with brine (25 mL). After the solvent was removed, hexane (50 mL) was added and the mixture was sonicated for 3 min. The white precipitates were filtered and washed with hexane (30 mL) to give the pure product (0.99 g, 60%).

5.1.2.1. 1-(4-Ethoxyphenyl)-2-(3,4,5-trimethoxyphenyl)ethanone (6a). Yield: 60%; ^{1}H NMR (400 MHz, DMSO-d_6): δ 1.34 (t, J = 7.2 Hz, 3H), 3.62 (s, 3H), 3.72 (s, 6H), 4.11 (q, J = 7.2 Hz, 2H), 4.23 (s, 2H), 6.58 (s, 2H), 7.02 (d, J = 8.4 Hz, 2H), 8.02(d, J = 8.4 Hz, 2H). MS (ESI), m/z: 331.16 $[M+H]^+$.

5.1.3. Procedure for the synthesis of 7a

The solution of 1-(4-ethoxyphenyl)-2-(3,4,5-trimethoxyphenyl)ethanone (496 mg, 1.5 mmol) dissolved in 10 mL anhydrous ether was placed in a 0 °C cold bath. Bromine (92 μL, 1.8 mmol) dissolved in 2 mL anhydrous ether was added by drop. After 40 min, the mixture was washed with water (3 × 10 mL), saturated aqueous sodium bicarbonate (3 × 10 mL), brine (3 × 10 mL) and dried with anhydrous sodium sulfate. After removal of the solvent, the residue was purified by flash chromatography using petroleum ether/ethyl acetate 5:1 (vol/vol) as the eluent to provide the desired product as a yellow solid (154 mg, 25.2%).

5.1.3.1. 2-Bromo-1-(4-ethoxyphenyl)-2-(3,4,5-trimethoxyphenyl)ethanone (7a). Yield: 25.2%; ^{1}H NMR (400 MHz, DMSO-d_6): δ 1.33 (t, J = 6.8 Hz, 3H), 3.65 (s, 3H), 3.75 (s, 6H), 4.12 (q, J = 8.8 Hz, 2H), 6.91 (s, 2H), 7.03 (d, J = 8.4 Hz, 2H), 7.06 (s, 1H), 8.06 (d, J = 8.4 Hz, 2H). MS (ESI), m/z: 408.92 $[M+H]^+$.

5.1.4. Procedure for the synthesis of 8a

The mixture of 2-bromo-1-(4-ethoxyphenyl)-2-(3,4,5-trimethoxyphenyl)ethanone (147 mg, 0.36 mmol) and thiourea (30 mg, 0.4 mmol) dissolved in anhydrous ethanol (10 mL) was refluxed for 3 h. After the solvent was removed under vacuo, saturated aqueous sodium bicarbonate was added to make the mixture basic (pH = 8–9). The mixture was then extracted with ethyl acetate (3 × 5 mL). The combined organic phase was washed with brine (5 mL) and dried with anhydrous sodium sulfate. After removal of the solvent, the residue was purified by flash chromatography using petroleum ether/ethyl acetate 1:1 (vol/vol) as the eluent to give the desired product as a white solid in 60% yield.

5.1.4.1. 4-(4-Ethoxyphenyl)-5-(3,4,5-trimethoxyphenyl)thiazol-2-amine (8a). Yield: 60%; mp: 178–181 °C. ^{1}H NMR (400 MHz, DMSO-d_6): δ 1.30 (t, J = 6.8 Hz, 3H), 3.61 (s, 6H), 3.66 (s, 3H), 4.00 (q, J = 7.2 Hz, 2H), 6.48 (s, 2H), 6.83 (d, J = 8.4 Hz, 2H), 7.08 (s, 2H), 7.36 (d, J = 8.4 Hz, 2H). ^{13}C NMR (100 MHz, DMSO-d_6): δ 15.24, 56.18, 60.32, 62.91, 106.31, 113.70, 117.83, 127.94, 128.62, 129.96, 136.46, 144.99, 152.86, 157.93, 165.66. MS (ESI), m/z: 387.1374 $[M+H]^+$.

5.1.5. Procedure for the synthesis of 8b

The mixture of 4-(4-ethoxyphenyl)-5-(3,4,5-trimethoxyphenyl)thiazol-2-amine (193 mg, 0.5 mmol) and Isopropyl nitrite (74 μL, 0.55 mmol) was dissolved in 5 mL DMF. After stirred at 80 °C for 3 h, 5 mL water was added and the mixture was extracted with ethyl acetate (3 × 5 mL). The combined organic phase was washed with brine (5 mL) and dried with anhydrous sodium sulfate. After removal of the solvent, the residue was purified by flash chromatography using petroleum ether/ethyl acetate 3:1 (vol/vol) as the eluent to give the desired product as a yellow solid in 50% yield.

5.1.5.1. 4-(4-Ethoxyphenyl)-5-(3,4,5-trimethoxyphenyl)thiazole (8b). Yield: 50%; mp: 95–98 °C. ^{1}H NMR (400 MHz, DMSO-d_6): δ 1.31 (t, J = 6.4 Hz, 3H), 3.65 (s, 6H), 3.69 (s, 3H), 4.02 (q, J = 6.4 Hz, 2H), 6.63 (s, 2H), 6.90 (d, J = 8.0 Hz, 2H), 7.44 (d, J = 8.4 Hz, 2H), 9.12 (s, 1H). ^{13}C NMR (100 MHz, DMSO-d_6): δ 14.43, 55.82, 60.19, 62.99, 106.63, 114.40, 126.74, 126.94, 129.84, 130.91, 137.54, 149.51, 152.19, 152.93, 158.20. MS (ESI), m/z: 372.1262 $[M+H]^+$.

5.1.6. General procedure for the synthesis of 8c–8e

The mixture of 2-bromo-1-(4-ethoxyphenyl)-2-(3,4,5-trimethoxyphenyl)ethanone (147 mg, 0.36 mmol) and replaced thiourea (0.4 mmol) in anhydrous ethanol (10 mL) was refluxed for 3 h. After that, the solvent was removed in vacuo, and saturated aqueous sodium bicarbonate was added to make the mixture basic (pH = 8–9). Then the mixture was extracted with ethyl acetate (3 × 5 mL). The combined organic phases were washed with brine (5 mL) and dried with anhydrous sodium sulfate. After removal of the solvent, the residue was purified by flash chromatography using petroleum ether/ethyl acetate 3:1 (vol/vol) as eluent, furnished product as solid.

5.1.6.1. 4-(4-Ethoxyphenyl)-5-(3,4,5-trimethoxyphenyl)-2-methylthiazole (8c). Yield: 61%; white solid; mp: 100–103 °C. ^{1}H NMR (400 MHz, DMSO-d_6): δ 1.07 (t, J = 6.8 Hz, 3H), 3.16 (s, 3H), 3.41 (s, 6H), 3.46 (s, 3H), 3.77 (q, J = 6.8 Hz, 2H), 6.36 (s, 2H), 6.64 (d, J = 8.4 Hz, 2H), 7.18 (d, J = 8.4 Hz, 2H). ^{13}C NMR (100 MHz, DMSO-d_6): δ 14.22, 18.71, 55.73, 60.05, 63.02, 106.24, 113.99, 126.93, 127.33, 129.81, 130.42, 137.46, 148.65, 153.23, 158.37, 162.93. MS (ESI), m/z: 386.1418 $[M+H]^+$.

5.1.6.2. 2-*tert*-Butyl-4-(4-ethoxyphenyl)-5-(3,4,5-trimethoxyphenyl)thiazole (8d). Yield: 58%; white solid; mp: 98–100 °C. ^{1}H NMR (400 MHz, DMSO-d_6): δ 1.31 (t, J = 6.8 Hz, 3H), 1.43 (s, 9H), 3.64 (s, 6H), 3.68 (s, 3H), 4.01 (q, J = 6.0 Hz, 2H), 6.60 (s, 2H), 6.88 (d, J = 8.0 Hz, 2H), 7.41 (d, J = 8.0 Hz, 2H). ^{13}C NMR (100 MHz, DMSO-d_6): δ 14.36, 30.54, 37.86, 55.78, 59.90, 62.63, 106.22, 113.84, 126.81, 127.15, 129.76, 129.96, 137.30, 148.05, 152.91, 157.95, 177.22. MS (ESI), m/z: 428.1889 $[M+H]^+$.

5.1.6.3. 2-(Diethoxymethyl)-4-(4-ethoxyphenyl)-5-(3,4,5-trimethoxyphenyl)thiazole (8e). Yield: 65%; white solid; mp: 102–105 °C. ^{1}H NMR (400 MHz, DMSO-d_6): δ 1.19 (t, J = 6.8 Hz, 6H), 1.30 (t, J = 6.8 Hz, 3H), 3.65 (s, 6H), 3.67 (s, 3H), 3.74 (q, J = 7.2 Hz, 4H), 4.00 (q, J = 6.8 Hz, 2H), 5.73 (s, 1H), 6.63 (s, 2H), 6.89 (d, J = 8.4 Hz, 2H), 7.41 (d, J = 8.4 Hz, 2H). ^{13}C NMR (100 MHz, DMSO-d_6): δ 14.51, 15.02, 55.76, 60.14, 61.81, 62.98, 98.38, 106.71, 114.06, 126.74, 129.84, 132.04, 137.48, 148.69, 152.87, 158.22, 165.85. MS (ESI), m/z: 474.1955$[M+H]^+$.

5.1.7. Procedure of method for the synthesis of 8f

The mixture of *N*-(diethoxymethyl)-4-(4-ethoxyphenyl)-5-(3,4,5-trimethoxyphenyl)thiazol-2-amine (98 mg, 0.2 mmol) and 1 N hydrochloric acid (10 mL) dissolved acetone (10 mL) was

heated at reflux for 3 h. After that, the solvent was removed in vacuo, and saturated aqueous sodium bicarbonate was added to make the mixture basic (pH = 8–9). Then the mixture was extracted with ethyl acetate (3 × 5 mL). The combined organic phases were washed with brine (5 mL) and dried with anhydrous sodium sulfate. After removal of the solvent, the residue was purified by flash chromatography using petroleum ether/ethyl acetate 3:1 (vol/vol) as eluent, furnished product as white solid (60 mg, 72%).

5.1.7.1. *N*-(4-(4-Ethoxyphenyl)-5-(3,4,5-trimethoxyphenyl)thiazol-2-yl)formamide (8f). Yield: 72%; white solid; mp: 150–153 °C. ^{1}H NMR (400 MHz, DMSO-d_6): δ 1.32 (t, J = 6.8 Hz, 3H), 3.65 (s, 6H), 3.70 (s, 3H), 4.05 (q, J = 6.8 Hz, 2H), 6.70 (s, 2H), 6.95 (d, J = 8.4 Hz, 2H), 7.45 (d, J = 8.4 Hz, 2H), 9.95 (s, 1H). ^{13}C NMR (100 MHz, DMSO-d_6): δ 14.43, 55.77, 60.08, 63.10, 106.84, 114.38, 125.50, 125.70, 129.96, 138.32, 139.38, 152.18, 152.72, 158.92, 162.36, 185.12. MS (ESI), m/z: 400.1218 [M+H]$^+$.

5.1.8. Procedure of method for the synthesis of 8g

The mixture of 2-bromo-1-(4-ethoxyphenyl)-2-(3,4,5-trimethoxyphenyl)ethanone (147 mg, 0.36 mmol) and ethyl thiocarbamoylformate (53.2 mg, 0.4 mmol) in anhydrous ethanol (10 mL) was heated at reflux for 3 h. After that, the solvent was removed in vacuo, and saturated aqueous sodium bicarbonate was added to make the mixture basic (pH = 8–9). Then the mixture was extracted with ethyl acetate (3 × 5 mL). The combined organic phases were washed with brine (5 mL) and dried with anhydrous sodium sulfate. After removal of the solvent, the residue was purified by flash chromatography using petroleum ether/ethyl acetate 3:1 (vol/vol) as eluent, furnished product as white solid (122 mg, 60%).

5.1.8.1. Ethyl 4-(4-ethoxyphenyl)-5-(3,4,5-trimethoxyphenyl) thiazole-2-carboxylate (8g). Yield: 60%; white solid; mp: 114–117 °C. ^{1}H NMR (400 MHz, DMSO-d_6): δ 1.30 (t, J = 7.2 Hz, 3H), 1.35 (t, J = 7.2 Hz, 3H), 3.65 (s, 6H), 3.70 (s, 3H), 4.03 (q, J = 6.8 Hz, 2H), 4.41 (q, J = 7.2 Hz, 2H), 6.68 (s, 2H), 6.94 (d, J = 8.4 Hz, 2H), 7.42 (d, J = 5.2 Hz, 2H). ^{13}C NMR (100 MHz, DMSO-d_6): δ 14.12, 14.51, 55.83, 60.16, 62.18, 63.07, 106.82, 114.24, 125.55, 125.94, 130.11, 113.90, 138.09, 151.16, 152.89, 153.82, 158.64, 162.22. MS (ESI), m/z: 444.1487 [M+H]$^+$.

5.1.9. Procedure of method for the synthesis of 9

The mixture of 2-bromo-2-(3,4,5-trimethoxyphenyl)-1-(4-methoxyphenyl)ethanone (142 mg , 0.36 mmol) and 2,2-diethoxyethanethioamide (65.2 mg , 0.4 mmol) in anhydrous ethanol (10 mL) was heated at reflux for 3 h. After that, the solvent was removed in vacuo, and saturated aqueous sodium bicarbonate was added to make the mixture basic (pH = 8–9). Then the mixture was extracted with ethyl acetate (3 × 5 mL). The combined organic phases were washed with brine (5 mL) and dried with anhydrous sodium sulfate. After removal of the solvent, the residue was purified by flash chromatography using petroleum ether/ethyl acetate 3:1 (vol/vol) as eluent, furnished product as white solid (111.6 mg, 60%).

5.1.9.1. 5-(3,4,5-Trimethoxyphenyl)-4-(4-methoxyphenyl)thiazol-2-amine (9). Yield: 60%; white solid; mp: 181–183 °C. ^{1}H NMR (400 MHz, DMSO-d_6): δ 3.61 (s, 6H), 3.65 (s, 3H), 3.73 (s, 3H), 6.47 (s, 2H), 6.85 (d, J = 8.4 Hz, 2H), 7.07 (s, 2H), 7.36 (d, J = 8.4 Hz, 2H). ^{13}C NMR (100 MHz, DMSO-d_6): δ 55.01, 55.80, 60.13, 106.42, 113.33, 117.83, 127.87, 128.60, 129.89, 136.33, 144.80, 152.93, 158.29, 165.86. MS (ESI), m/z: 373.1216 [M+H]$^+$.

5.1.10. General procedure of method for the synthesis of 10a–10d

The mixture of 4-(4-ethoxyphenyl)-5-(3,4,5-trimethoxyphenyl) thiazol-2-amine (193 mg, 0.5 mmol) and RI (1.0 equiv) was dissolved in 5 mL tetrahydrofuran. Sodium hydride (24 mg, 1 mmol) was added and stirred at room temperature for 3 h. Then water (5 mL) was added and extracted with ethyl acetate (3 × 5 mL). The combined organic phases were washed with brine (10 mL) and dried with anhydrous anhydrous sodium sulfate. After removal of the solvent, the residue was purified by flash chromatography using petroleum ether/ethyl acetate 3:1 (vol/vol) as eluent, furnished product as oil.

5.1.10.1. 4-(4-Ethoxyphenyl)-5-(3,4,5-trimethoxyphenyl)-*N*,*N*-dimethylthiazol-2-amine (10a). Yield: 48%; yellow oil. ^{1}H NMR (400 MHz, DMSO-d_6): δ 1.30 (t, J = 6.8 Hz, 3H), 3.06 (s, 6H), 3.60 (s, 6H), 3.65 (s, 3H), 4.01 (q, J = 6.8 Hz, 2H), 6.48 (s, 2H), 6.86 (d, J = 8.0 Hz, 2H), 7.38 (d, J = 8.4 Hz, 2H). ^{13}C NMR (100 MHz, DMSO-d_6): δ 14.1, 39.6, 55.5, 60.1, 62.9, 106.1, 113.89, 118.6, 127.8, 128.1, 129.8, 136.6, 145.9, 152.7, 157.7, 167.2. MS (ESI), m/z: 415.1692 [M+H]$^+$.

5.1.10.2. 4-(4-Ethoxyphenyl)-*N*,*N*-diethyl-5-(3,4,5-trimethoxyphenyl)thiazol-2-amine (10b). Yield: 48%; yellow oil. ^{1}H NMR (400 MHz, DMSO-d_6): δ 1.19 (d, J = 7.2 Hz, 6 H), 1.30 (d, J = 6.8 Hz, 3H), 3.47 (q, J = 6.8 Hz, 4H), 3.60 (s, 6H), 3.65 (s, 3H), 4.00 (q, J = 6.8 Hz, 2H), 6.48 (s, 2H), 6.85 (d, J = 8.0 Hz, 2H), 7.37 (d, J = 8.0 Hz, 2H). ^{13}C NMR (100 MHz, DMSO-d_6): δ 12.5, 14.5, 44.7, 55.6, 60.0, 62.9, 106.2, 113.8, 117.3, 127.8, 128.1, 129.8, 136.4, 145.6, 152.7, 157.8, 165.3. MS (ESI), m/z: 443.1996 [M+H]$^+$.

5.1.10.3. 4-(4-Ethoxyphenyl)-5-(3,4,5-trimethoxyphenyl)-*N*,*N*-dipropylthiazol-2-amine (10c). Yield: 52%; yellow oil. ^{1}H NMR (400 MHz, DMSO-d_6): δ 0.90 (d, J = 7.2 Hz, 6H), 1.30 (d, J = 6.8 Hz, 3H), 1.69 (m, 4H), 3.67 (t, J = 6.0 Hz, 4H), 3.60 (s, 6H), 3.65 (s, 3H), 4.08 (q, J = 6.8 Hz, 2H), 6.49 (s, 2H), 6.86 (d, J = 8.0 Hz, 2H), 7.37 (d, J = 8.4 Hz, 2H). ^{13}C NMR (100 MHz, DMSO-d_6): δ 11.1, 14.6, 20.1, 52.3, 55.5, 60.0, 63.0, 106.2, 114.2, 117.1, 127.7, 128.2, 129.8, 136.4, 145.2, 152.5, 157.6, 166.0. MS (ESI), m/z: 471.2283 [M+H]$^+$.

5.1.10.4. *N*,*N*-Diallyl-4-(4-ethoxyphenyl)-5-(3,4,5-trimethoxyphenyl)thiazol-2-amine (10d). Yield: 50.6%; yellow oil. ^{1}H NMR (400 MHz, DMSO-d_6): δ 1.30 (t, J = 6.8 Hz, 3H), 3.61 (s, 6H), 3.65 (s, 3H), 4.00 (q, J = 6.8 Hz, 2H), 4.07 (d, J = 5.2 Hz, 4H), 5.22 (s, 1H), 5.23 (s, 2H), 5.28 (s, 1H), 5.89 (m, 1H), 6.49 (s, 2H), 6.85 (d, J = 8.0 Hz, 2H), 7.38 (d, J = 8.0 Hz, 2H). ^{13}C NMR (100 MHz, DMSO-d_6): δ 14.5, 52.3, 55.6, 60.0, 62.9, 106.3, 113.8, 117.6, 118.3, 127.6, 127.9, 129.8, 132.8, 136.6, 145.2, 152.8, 157.8, 165.7. MS (ESI), m/z: 467.2012 [M+H]$^+$.

5.1.11. General procedure of method for the synthesis of 10e–10h

The material of 4-(4-ethoxyphenyl)-5-(3,4,5-trimethoxyphenyl)thiazol-2-amine (193 mg, 0.5 mmol) was dissolved in 10 mL $R(CO)_2O$. The mixture was refluxed for 3 h. Water (10 mL) was added and saturated aqueous sodium bicarbonate was added to make the mixture basic (pH = 8–9). Then the mixture was extracted with ethyl acetate (3 × 10 mL). The combined organic phases were washed with brine (10 mL) and dried with anhydrous anhydrous sodium sulfate. After removal of the solvent, the residue was purified by flash chromatography using petroleum ether/ethyl acetate 3:1 (vol/vol) as eluent, furnished product as white solid.

5.1.11.1. *N*-(4-(4-Ethoxyphenyl)-5-(3,4,5-trimethoxyphenyl)thiazol-2-yl)acetamide (10e). Yield: 42%; white solid; mp: 170–172 °C. ^{1}H NMR (400 MHz, DMSO-d_6): δ 1.31 (t, J = 6.8 Hz, 3H), 2.17 (s, 3H), 3.64 (s, 6H), 3.68 (s, 3H), 4.01 (q, J = 7.2 Hz, 2H), 6.58 (s, 2H), 6.89 (d, J = 4.0 Hz, 2H), 7.40 (d, J = 8.4 Hz, 2H), 12.23 (s, 1H).^{13}C NMR (100 MHz, DMSO-d_6): δ 14.5, 20.9, 2.3, 55.7, 60.0, 62.9, 106.6, 114.0, 123.8, 127.0, 127.4, 129.7, 137.1, 143.4, 152.9, 155.2, 157.9, 168.5, 171.9. MS (ESI), m/z: 429.1468 [M+H]$^+$.

5.1.11.2. *N*-(4-(4-Ethoxyphenyl)-5-(3,4,5-trimethoxyphenyl)thiazol-2-yl)propionamide (10f). Yield: 43%; white solid; mp: 167–169 °C. ^{1}H NMR (400 MHz, DMSO-d_6): δ 1.11 (t, J = 7.6 Hz, 3H), 1.31 (t, J = 7.2 Hz, 3H), 2.46 (t, J = 7.6 Hz, 2H), 3.65 (s, 6H), 3.69 (s, 3H), 4.01 (q, J = 6.8 Hz, 2H), 6.58 (s, 2H), 6.89 (d, J = 4.4 Hz, 2H), 7.41 (d, J = 8.4 Hz, 2H), 12.19 (s, 1H). ^{13}C NMR (100 MHz, DMSO-d_6): δ 8.8, 14.5, 28.2, 55.7, 60.1, 62.9, 106.5, 114.3, 123.8, 127.0, 127.5, 129.8, 137.0, 143.5, 152.7, 155.6, 158.0, 172.2. MS (ESI), m/z: 443.1637 [M+H]$^+$.

5.1.11.3. *N*-(4-(4-Ethoxyphenyl)-5-(3,4,5-trimethoxyphenyl)thiazol-2-yl)butyramide (10g). Yield: 43%; white solid; mp: 150–153 °C. ^{1}H NMR (400 MHz, DMSO-d_6): δ 0.91 (s, 3H), 1.30 (s, 3H), 1.64 (d, J = 6.4 Hz, 2H), 2.43 (s, 2H), 3.64 (s, 6H), 3.68 (s, 3H), 4.01 (d, J = 6.4 Hz, 2H), 6.58 (s, 2H), 6.88 (d, J = 7.2 Hz, 2H), 7.40 (d, J = 6.8 Hz, 2H), 12.21 (s, 1H). ^{13}C NMR (100 MHz, DMSO-d_6): δ 13.4, 14.5, 18.2, 36.7, 55.7, 60.0, 62.9, 106.5, 114.0, 123.8, 127.0, 127.4, 129.7, 137.0, 143.4, 152.9, 155.2, 157.9, 171.3. MS (ESI), m/z: 457.1789[M+H]$^+$.

5.1.11.4. *N*-(4-(4-Ethoxyphenyl)-5-(3,4,5-trimethoxyphenyl)thiazol-2-yl)acetamide (10h). Yield: 40%; white solid; mp: 130–133 °C. ^{1}H NMR (400 MHz, DMSO-d_6): δ 1.31 (t, J = 6.8 Hz, 3H), 1.34 (d, J = 6.8 Hz, 6H), 2.75 (m, 1H), 3.64 (s, 6H), 3.68 (s, 3H), 4.01 (q, J = 6.8 Hz, 2H), 6.58 (s, 2H), 6.89 (d, J = 4.4 Hz, 2H), 7.40 (d, J = 8.4 Hz, 2H), 12.20 (s, 1H). ^{13}C NMR (100 MHz, DMSO-d_6): δ 14.5, 19.0, 33.7, 55.5, 60.0, 62.9, 106.6, 14.0, 123.9, 127.0, 127.4, 129.7, 137.1, 143.4, 152.9, 155.3, 157.9, 175.4, 181.1. MS (ESI), m/z: 457.1802 [M+H]$^+$.

5.1.12. Procedure of method for the synthesis of 10i

The mixture of 4-(4-ethoxyphenyl)-5-(3,4,5-trimethoxyphenyl) thiazol-2-amine (193 mg, 0.5 mmol) and 1-(bromomethyl)benzene (1.0 equiv) was dissolved in 5 mL tetrahydrofuran. Sodium hydride (24 mg, 1 mmol) was added and stirred at room temperature for 3 h. Then 5 mL water was added and extracted with ethyl acetate (3 × 5 mL). The combined organic phases were washed with brine (10 mL) and dried with anhydrous sodium sulfate. After removal of the solvent, the residue was purified by flash chromatography using petroleum ether/ethyl acetate 3:1 (vol/vol) as eluent, furnished product as white solid.

5.1.12.1. *N,N*-Dibenzyl-4-(4-ethoxyphenyl)-5-(3,4,5-trimethoxyphenyl)thiazol-2-amine (10i). Yield: 48%; white solid; mp: 126–129 °C. ^{1}H NMR (400 MHz, DMSO-d_6): δ 1.35 (t, J = 6.8 Hz, 3H), 3.65 (s, 6H), 3.70 (s, 3H), 4.05 (q, J = 6.4 Hz, 2H), 4.78 (s, 4H), 6.55 (s, 2H), 6.90 (d, J = 8.0 Hz, 2H), 7.35 (s, 1H), 7.36 (s, 1H), 7.39 (m, 1H), 7.40 (s, 3H), 7.42 (s, 1H), 7,45 (s, 1H), 7.47 (s, 1H). ^{13}C NMR (100 MHz, DMSO-d_6): δ 14.5, 53.5, 55.6, 60.0, 62.9, 106.4, 113.9, 118.4, 127.3, 127.4, 127.5, 127.8, 128.5, 129.8, 136.6, 136.9, 145.2, 156.2, 157.8, 166.5. MS (ESI), m/z: 567.2317 [M+H]$^+$.

5.1.13. Procedure of method for the synthesis of 10j

The material of 4-(4-ethoxyphenyl)-5-(3,4,5-trimethoxyphenyl)thiazol-2-amine (193 mg, 0.5 mmol) and substituted isocyanate (78 μL, 1 mmol) was dissolved in 10 mL dichloromethane. The solution was stirred for 3 h. After removal of the solvent, the residue was purified by flash chromatography using petroleum ether/ethyl acetate 3:1 (vol/vol) as eluent, furnished product as white solid.

5.1.13.1. 1-(4-(4-Ethoxyphenyl)-5-(3,4,5-trimethoxyphenyl)thiazol-2-yl)-3-ethylurea (10j). Yield: 36%; white solid; mp: 165–167 °C. ^{1}H NMR (400 MHz, DMSO-d_6): δ 1.08 (t, J = 7.2 Hz, 3H), 1.30 (t, J = 6.8 Hz, 3H), 3.17 (m, 1H), 3.64 (s, 6H), 3.68 (s, 3H), 4.01 (q, J = 7.2 Hz, 2H), 6.50 (s, 1H), 6.55 (s, 2H), 6.87 (d, J = 8.8 Hz, 2H), 6.38 (d, J = 8.8 Hz, 2H), 10.53 (s, 1H). ^{13}C NMR (100 MHz, DMSO-d_6): δ 14.5, 15.1, 34.2, 55.7, 60.0, 62.9, 106.4, 113.9, 122.5, 127.2, 127.8, 129.6, 136.8, 143.1, 152.9, 153.7, 157.2, 157.8. MS (ESI), m/z: 458.1755 [M+H]$^+$.

5.1.14. General procedure of method for the synthesis of 10k–10o

The mixture of 4-(4-ethoxyphenyl)-5-(3,4,5-trimethoxyphenyl)thiazol-2-amine (193 mg, 0.5 mmol) and RSO_2Cl (1.0 equiv) was dissolved in 5 mL tetrahydrofuran. Sodium hydride (24 mg, 1 mmol) was added and stirred at room temperature for 3 h. Then 5 mL water was added and extracted with ethyl acetate (3 × 5 mL). The combined organic phases were washed with brine (10 mL) and dried with anhydrous sodium sulfate. After removal of the solvent, the residue was purified by flash chromatography using petroleum ether/ethyl acetate 3:1 (vol/vol) as eluent, furnished product as yellow solid.

5.1.14.1. *N*-(4-(4-Ethoxyphenyl)-5-(3,4,5-trimethoxyphenyl)thiazol-2-yl)-3-fluoro-4-methoxybenzenesulfonamide (10k). Yield: 50.6%; yellow solid; mp: 110–113 °C. ^{1}H NMR (400 MHz, DMSO-d_6): δ 1.30 (t, J = 6.8 Hz, 3H), 3.60 (s, 6H), 3.64 (s, 3H), 3.90 (s, 3H), 4.03 (q, J = 6.8 Hz, 2H), 6.48 (s, 2H), 6.94 (d, J = 8.4 Hz, 2H), 7.29 (d, J = 8.4 Hz, 2H), 7.34 (d, J = 8.4 Hz, 1H), 7.62 (d, J = 8.8 Hz, 1H), 13.08 (s, 1H). ^{13}C NMR (100 MHz, DMSO-d_6): δ 14.48, 55.60, 56.43, 60.16, 63.33, 106.01, 113.45, 113.75, 114.71, 116.89, 123.12, 125.65, 130.46, 137.31, 149.39, 150.10, 152.87, 189.49. MS (ESI), m/z: 575.1320 [M+H]$^+$.

5.1.14.2. *N*-(4-(4-Ethoxyphenyl)-5-(3,4,5-trimethoxyphenyl)thiazol-2-yl)-2-methoxy-4-nitrobenzenesulfonamide (10l). Yield: 47%; yellow solid; mp: 122–125 °C. ^{1}H NMR (400 MHz, DMSO-d_6): δ 1.30 (t, J = 7.6 Hz, 3H), 3.61 (s, 6H), 3.65 (s, 3H), 3.96 (s, 3H), 4.03 (q, J = 7.2 Hz, 2H), 6.50 (s, 2H), 6.95 (d, J = 7.2 Hz, 2H), 7.31 (d, J = 7.2 Hz, 2H), 7.94 (m, 2H), 8.10 (d, J = 8.8 Hz, 2H), 13.23 (s, 1H). ^{13}C NMR (100 MHz, DMSO-d_6): δ 14.48, 55.82, 56.89, 59.97, 63.20, 106.02, 107.79, 114.42, 115.01, 117.84, 120.87, 126.10, 129.83, 130.59, 135.33, 137.64, 150.64, 153.23, 157.27, 159.34, 167.04. MS (ESI), m/z: 602.1268 [M+H]$^+$.

5.1.14.3. 4-Bromo-*N*-(4-(4-ethoxyphenyl)-5-(3,4,5-trimethoxyphenyl)thiazol-2-yl)-2-(trifluoromethyl)benzenesulfonamide (10m). Yield: 48%; yellow solid; mp: 125–128 °C. ^{1}H NMR (400 MHz, DMSO-d_6): δ 1.30 (t, J = 7.6 Hz, 3H),3.60 (s, 6H), 3.64 (s, 3H), 4.03 (q, J = 7.8 Hz, 2H), 6.48 (s, 2H), 6.95 (d, J = 8.4 Hz, 2H), 7.30 (d, J = 8.4 Hz, 2H), 8.10 (s, 1H), 8.13 (d, J = 4.4 Hz, 1H), 8.17 (d, J = 8.4 Hz, 1H), 13.30 (s, 2H). ^{13}C NMR (100 MHz, DMSO-d_6): δ 14.36, 55.37, 60.05, 63.25, 106.12, 114.48, 118.02, 120.59, 125.42, 125.94, 130.48, 130.93, 131.98, 134.16, 136.09, 137.59, 140.12, 153.33, 160.30, 165.85. MS (ESI), m/z: 673.0294[M+H]$^+$.

5.1.14.4. *N*-(4-(4-Ethoxyphenyl)-5-(3,4,5-trimethoxyphenyl)thiazol-2-yl)-3,4-dimethylbenzenesulfonamide (10n). Yield: 49%; yellow solid; mp: 115–117 °C. ^{1}H NMR (400 MHz, DMSO-d_6): δ 1.30 (t, J = 6.8 Hz, 3H), 2.34 (s, 6H), 3.60 (s, 6H), 3.65 (s, 3H), 4.02 (q, J = 7.2 Hz, 2H), 6.48 (s, 2H), 6.94 (d, J = 8.4 Hz, 2H), 7.25 (s, 1H), 7.28 (s, 1H), 7.30 (s, 1H), 7.47 (s, 2H), 12.99 (s, 1H).

^{13}C NMR (100 MHz, DMSO-d_6): δ 14.58, 20.73, 55.90, 59.96, 63.27, 106.10, 106.28, 113.91, 114.49, 123.35, 125.79, 129.98, 130.35, 133.59, 137.36, 138.62, 142.03, 152.83, 152.95, 159.18. MS (ESI), m/z: 555.1630 $[M+H]^+$.

5.1.14.5. 2-Chloro-*N*-(4-(4-ethoxyphenyl)-5-(3,4,5-trimethoxyphenyl)thiazol-2-yl)thiophene-3-sulfonamide (10o). Yield: 46.6%; yellow solid; mp: 129–131 °C. ^{1}H NMR (400 MHz, DMSO-d_6): δ 0.85 (s, 1H), 1.31 (t, J = 6.8 Hz, 3H), 3.60 (s, 6H), 3.65 (s, 3H), 4.04 (q, J = 6.8 Hz, 2H), 6.50 (s, 2H), 6.96 (d, J = 8.4 Hz, 2H), 7.32 (d, J = 8.4 Hz, 2H), 7.38 (s, 1H), 13.36 (s, 1H). ^{13}C NMR (100 MHz, DMSO-d_6): δ 14.19, 55.78, 60.41, 63.10, 106.04, 114.43, 117.92, 120.36, 125.54, 125.88, 126.78, 127.71, 130.69, 137.61, 152.97, 159.47, 166.57. MS (ESI), m/z: 567.0492 $[M+H]^+$.

5.1.14.6. 4-(3,4,5-Trimethoxyphenyl)-5-(4-ethoxyphenyl)thiazol-2-amine (3n). The 4-(3,4,5-trimethoxyphenyl)-5-4-ethoxyphenyl) thiazol-2-amine was repeated by the routes of Viola.[18] ^{1}H NMR (400 MHz, DMSO-d_6): δ 1.31 (t, J = 6.8 Hz, 3H), 3.40 (s, 6H), 3.53 (s, 3H), 4.01 (q, J = 6.8 Hz, 2H), 6.68 (s, 2H), 6.90 (d, J = 8.8 Hz, 2H), 7.09 (br s, 2H), 7.22 (d, J = 8.8 Hz, 2H).

5.2. Biological assay methods

5.2.1. Antiproliferative assays

HCT116, HepG2, SMMC-7721, SK-OV-3, A2780s cells were cultured in DMEM (Gibco, Milano, Italy). A549, A549/T, MCF-7, MCF-7/ADR, HCC827, H1975 cells were cultured in RPMI-1640 medium (Gibco, Milano, Italy). All media contained 10% fetal bovine serum (FBS) (Invitrogen, Milano, Italy), 100 units/mL penicillin (Gibco, Milano, Italy), and 100 μg/mL streptomycin (Gibco, Milano, Italy). Human umbilical vein endothelial cells (HUVEC) were isolated from human umbilical cord veins by a procedure as previously described,[28,29] and grown in EBM-2 medium containing the essential growth factors. Cells were incubated at 37 °C in a humidified atmosphere of 5% CO_2. Cells in logarithmic phase were diluted to a density of 40,000–50,000 cells/mL in culture medium and treated with various concentrations of compounds in 96-well culture plates for 48 h in final volumes of 200 μL. Then 20 μL MTT (5 mg/mL) was added to each well, and the cells were incubated for an additional 3 h. After carefully removing the medium, the precipitates were dissolved in 150 μL of DMSO, shaken mechanically for 5 min, and then absorbance values at a wavelength of 570 nm were taken on a spectrophotometer (Molecular Devices, Sunnyvale, USA). IC_{50} values were calculated using percentage of growth versus untreated control.

5.2.2. Tubulin polymerization assay

Turbidimetric assays of microtubules were generally performed as described, with some modification.[30] Microtubule protein was purchased (Cytoskeleton Inc.) or purified from porcine brain by our team following the method described.[31] MAP-rich tubulin (3 mg/mL) was preincubated in the polymerization buffer (0.1 M PIPES, pH 6.9, 2 mM $MgCl_2$, 0.5 mM EGTA) at 4 °C for 30 min while the 96-well plate was pre-warmed to 37 °C. 2 min before the start of the measurement, various compounds at the indicated concentrations were added to the wells. Then, 1 mM guanosine triphosphate (GTP) was added to the tubulin and mixed. The tubulin-containing sample was rapidly diluted into the 96-well plate (100 μL per well). Immediately, the change in absorbance at 340 nm was kinetically measured at 37 °C by a thermostatically controlled spectrophotometer. The microtubule assembly IC_{50} values were calculated using the method described by Hamel.[30]

5.2.3. EBI competition assay

The EBI competition assay was generally conducted as the same method reported previously,[25] with some modifications. HepG2 cells were seeded in 6-well plates at 500,000 cells/well. After cell adherence, compounds were added to the cells for 4 h. Then, EBI (purchased from TRC Biomedical Research Chemicals, Canada) was added at 100 μM and incubated for 1.5 h. Thereafter, the cells were harvested and cell extracts were prepared for Western blot analysis. Equivalent samples (about 20 μg of protein) were subjected to SDS–PAGE using 10% polyacrylamide gels (SDS was at the purity of 95%). Then, proteins were transferred to PVDF membranes. After blocking by 5% non-fat milk for 1 h, the membranes were incubated with anti-β-tubulin antibody (Cell Signaling Technology, #2146) and subsequently probed by the secondary antibody conjugated to horseradish peroxidase. Immunoreactive bands were visualized using enhanced chemiluminescence (Millipore, USA). GAPDH was also examined to approve equal loading of protein.

5.2.4. Flow cytometry

Flow cytometry analysis of cell cycle and apoptosis were generally handled as the same method previously described.[26] HepG2 cells were treated with various concentrations of **8a** or DMSO vehicle for 24 or 48 h. Cells were harvested by trypsinization. The cells were washed twice by PBS, then followed the staining with 50 μg/ml PI containing 1 mg/mL of DNase-free RNase to analyze cell cycle, or dual staining with PI & Annexin-V to measure cell apoptosis. The cells were finally analyzed by flow cytometer (TASC240, USA). The cell cycle distribution was further analyzed using the MODFIT3.2 software.

5.2.5. Immunofluorescence staining of tubulin

HepG2 cells were seeded into 6-well plates, then treated as indicated for 16 h. The cells were fixed with 4% paraformaldehyde and then penetrated with PBS containing 0.5% Triton X-100. After blocking for 30 min in 5% goat serum albumin at room temperature, cells were incubated with a monoclonal anti-α-tubulin antibody at room temperature for 1 h. Then the cells was washed 3 times by PBS following staining by fluorescence antibody and labeling of Nuclei by 4,6-diamidino-2-phenylindole (DAPI). Cells were finally washed thrice and visualized using a fluorescence microscope (OLYMPUS).

5.2.6. Molecular docking

The simulation system was built based on the X-ray crystal structure of the protein, which was obtained from the Protein Data Bank (PDB 1SA0; www.rcsb.org) and further modified for the docking calculations.

Water molecules were removed and H atoms were added to the structure. 3D structures of the compounds were generated and optimized by the Discovery Studio 3.1 (Accelrys, San Diego, CA, USA). The receptor-grid files were carried out using a grid-receptor generation program using default settings after ensuring that the ligands and the protein are in correct form. The GOLD program in the Discovery Studio software was used to perform the docking simulations, which allows full flexibility of the ligand.

5.2.7. Wound-healing assay

HUVECs were seeded in 6-well plates, and grown overnight to reach a monolayer of confluence. The cells were wounded by scratching with pipet tips and washed twice by PBS to remove the non-adherent cells. Fresh EBM2 medium containing vehicle or different concentrations of **8a** was added. Images were taken by an inverted fluorescence microscopy (Olympus) after 24 h. The migrated cells were quantified by manual counting.

5.2.8. Tube formation assay

Matrigel was dissolved at 4 °C overnight. Each well of pre-chilled 96-well plates was coated with 50 μL of Matrigel, following incubation and solidification at 37 °C for 45 min. HUVECs at the density of 1×10^4 in EBM-2 containing the indicated concentrations of **8a** were seeded into the wells. After 8 h, images were digitally captured (Olympus). The numbers and line lengths of the circular tubules formed by the cells were calculated manually.

5.2.9. Antitumor activity in vivo

5 to 6-week-old female Balb/C athymic nude mice purchased from the animal breeding laboratories at Sichuan University Animal Center (Sichuan, Chengdu, China) were implanted the indicated number of cells suspended in 100 μL HBSS into the right flank. Ten days after the average tumor volume reached 100 mm^3, twenty-four mice were randomly divided into four groups: vehicle control group, 5-FU (10 mg/kg) treatment group, **8a** (20 mg/kg) treatment group, **8a** (50 mg/kg) treatment group. Treatment was conducted with 5-FU injected intraperitoneally daily at the dose of 10 mg/kg or **8a** injected intraperitoneally daily at doses of 20 mg/kg or 50 mg/kg. Length and width of the tumors were measured, and the tumor volume (mm^3) was calculated by the formula: $\pi/6 \times \text{length} \times \text{width}^2$. Tumor volumes and body weights were measured every two days. The antitumor activity of compound was evaluated by tumor inhibition = (1 − tumor weight of treat group/tumor weight of control group) × 100%.

Acknowledgments

The authors greatly appreciate the financial support from National Key Programs of China during the 12th Five-Year Plan Period (2012ZX09103101-009), and National Natural Science Foundation of China (81373283).

Supplementary data

Supplementary data (the ^1H spectra, ^{13}C spectra, Mass spectrogram of **8a**. The figures of cell cycle and cell apoptosis analysis in HepG2 cells. The mice body weight figures of in vivo antitumor activity) associated with this article can be found, in the online version, at http://dx.doi.org/10.1016/j.bmc.2015.04.055.

References

1. Romagnoli, R.; Baraldi, P. G.; Cruz-Lopez, O. *J. Med. Chem.* **2010**, *53*, 4248.
2. Stefely, J. A.; Palchaudhuri, R.; Miller, P. A.; Peterson, R. J.; Moraski, G. C.; Hergenrother, P. J.; Miller, M. J. *J. Med. Chem.* **2010**, *53*, 3389.
3. Ravelli, R. B.; Gigant, B.; Curmi, P. A.; Jourdain, I.; Lachkar, S.; Sobel, A.; Knossow, M. *Nature* **2004**, *428*, 198.
4. Kavallaris, M. *Nat. Rev. Cancer* **2010**, *10*, 194.
5. Wilson, L.; Jordan, M. A. *J. Chemother.* **2004**, *16*, 83.
6. Liou, J. P.; Wu, C. Y.; Hsieh, H. P.; Chang, C. Y.; Chen, C. M.; Kuo, C. C.; Chang, J. Y. *J. Med. Chem.* **2007**, *50*, 4548.
7. Tron, G. C.; Pagliai, F.; Del Grosso, E.; Genazzani, A. A.; Sorba, G. *J. Med. Chem.* **2005**, *48*, 3260.
8. Srivastava, V.; Negi, A. S.; Kumar, J. K.; Gupta, M. M.; Khanuja, S. P. *Bioorg. Med. Chem.* **2005**, *13*, 5892.
9. Lawrence, N. J.; Patterson, R. P.; Ooi, L. L.; Cook, D.; Ducki, S. *Bioorg. Med. Chem. Lett.* **2006**, *16*, 5844.
10. Tron, G. C.; Pirali, T.; Sorba, G.; Pagliai, F.; Busacca, S.; Genazzani, A. A. *J. Med. Chem.* **2006**, *49*, 3033.
11. Canela, M. D.; Perez-Perez, M. J.; Noppen, S.; Saez-Calvo, G.; Diaz, J. F.; Camarasa, M. J.; Liekens, S.; Priego, E. M. *J. Med. Chem.* **2014**, *57*, 3924.
12. Lippert, J. W., 3rd *Bioorg. Med. Chem.* **2007**, *15*, 605.
13. Siemann, D. W. *Cancer Treat. Rev.* **2011**, *37*, 63.
14. Wang, X. F.; Guan, F.; Ohkoshi, E.; Guo, W.; Wang, L.; Zhu, D. Q.; Wang, S. B.; Wang, L. T.; Hamel, E.; Yang, D.; Li, L.; Qian, K.; Morris-Natschke, S. L.; Yuan, S.; Lee, K. H.; Xie, L. *J. Med. Chem.* **2014**, *57*, 1390.
15. Kingston, D. G. I. *J. Nat. Prod.* **2009**, *72*, 507.
16. Zhang, Q.; Peng, Y.; Wang, X. I.; Keenan, S. M.; Arora, S.; Welsh, W. J. *J. Med. Chem.* **2007**, *50*, 749.
17. Romagnoli, R.; Baraldi, P. G.; Salvador, M. K.; Prencipe, F.; Bertolasi, V.; Cancellieri, M.; Brancale, A.; Hamel, E.; Castagliuolo, I.; Consolaro, F.; Porcu, E.; Basso, G.; Viola, G. *J. Med. Chem.* **2014**, *57*, 6795.
18. Romagnoli, R.; Baraldi, P. G.; Brancale, A.; Ricci, A.; Hamel, E.; Bortolozzi, R.; Basso, G.; Viola, G. *J. Med. Chem.* **2011**, *54*, 5144.
19. Romagnoli, R.; Baraldi, P. G.; Salvador, M. K.; Preti, D. *J. Med. Chem.* **2012**, *55*, 475.
20. Davlieva, M. G.; Lindeman, S. V.; Neretin, I. S.; Kochi, J. K. *J. Org. Chem.* **2005**, *70*, 4013.
21. Shaikh, T. M.; Sudalai, A. *Tetrahedron Lett.* **2005**, *46*, 5589.
22. Huey, R.; Morris, G. M.; Olson, A. J.; Goodsell, D. S. *J. Comput. Chem.* **2007**, *28*, 1145.
23. Fortin, S.; Lacroix, J.; Cote, M. F.; Moreau, E.; Petitclerc, E. *Online* **2010**, *12*, 113.
24. Mukhtar, E.; Adhami, V. M.; Mukhtar, H. *Mol. Cancer Ther.* **2014**, *13*, 275.
25. Jordan, M. A.; Wilson, L. *Nat. Rev. Cancer* **2004**, *4*, 253.
26. Yang, Z.; Wu, W.; Wang, J.; Liu, L.; Li, L.; Yang, J.; Wang, G.; Cao, D.; Zhang, R.; Tang, M.; Wen, J.; Zhu, J.; Xiang, W.; Wang, F.; Ma, L.; Xiang, M.; You, J.; Chen, L. *J. Med. Chem.* **2014**, *57*, 7977.
27. Szakacs, G.; Paterson, J. K.; Ludwig, J. A.; Booth-Genthe, C.; Gottesman, M. M. *Nat. Rev. Drug Disc.* **2006**, *5*, 219.
28. Zhang, S.; Cao, Z.; Tian, H.; Shen, G.; Ma, Y.; Xie, H.; Liu, Y.; Zhao, C.; Deng, S.; Yang, Y.; Zheng, R.; Li, W.; Zhang, N.; Liu, S.; Wang, W.; Dai, L.; Shi, S.; Cheng, L.; Pan, Y.; Feng, S.; Zhao, X.; Deng, H.; Yang, S.; Wei, Y. *Clin. Cancer Res.* **2011**, *17*, 4439.
29. Wang, G.; Wang, F.; Cao, D.; Liu, Y.; Zhang, R.; Ye, H.; Li, X.; He, L.; Yang, Z.; Ma, L.; Peng, A.; Xiang, M.; Wei, Y.; Chen, L. *Bioorg. Med. Chem. Lett.* **2014**, *24*, 3158.
30. Hamel, E. *Cell Biochem. Biophys.* **2003**, *38*, 1.
31. Gell, C.; Friel, C. T.; Borgonovo, B.; Drechsel, D. N.; Hyman, A. A.; Howard, J. *Purification of Tubulin from Porcine Brain*. **2011**, *777*, 15.